Inorg. Chem. **1982**, *21*, 1864–1872

Contribution from Ames Laboratory[1] and the Department of Chemistry,
Iowa State University, Ames, Iowa 50011

Sulfur-Substituted Derivatives of the Octa-μ_3-chloro-hexamolybdenum(4+) Cluster Unit. Synthesis and Structure of Two Salts Containing the Hexachlorohepta-μ_3-chloro-μ_3-sulfido-hexamolybdenum(3−) Anion

JOHN B. MICHEL and ROBERT E. McCARLEY*

Received July 7, 1981

A synthetic procedure has been devised for stepwise displacement of chloride by sulfide in the $Mo_6Cl_8^{4+}$ cluster via reaction of Mo_6Cl_{12} with NaSH in refluxing pyridine. The $(Mo_6Cl_7S)^{3+}$ cluster has been isolated in two different salts containing the chloro anion $[(Mo_6Cl_7S)Cl_6]^{3-}$, and the structures have been determined by X-ray diffraction. $(C_5H_5NH)_3[(Mo_6Cl_7S)Cl_6]$ (I) crystallizes in the space group $P2_1/c$ with $a = 13.469$ (4) Å, $b = 15.329$ (3) Å, $c = 17.115$ (5) Å, $\beta = 107.19$ (3)°, and $Z = 4$. With excess pyridinium ion present in solution, the cubic double salt $(C_5H_5NH)_3[(Mo_6Cl_7S)Cl_6]\cdot 3(C_5H_5NH)Cl$ (II) is obtained: space group $Pa3$, with $a = 17.158$ (2) Å and $Z = 4$. Bond distances obtained after refinement of the two structures indicate sulfide is probably disordered over only two bridging ligand sites in I but over all eight sites in II. Corresponding average bond distances and angles in the two structures are in close agreement. Similarly, infrared spectra for I and II are in good agreement; a band appearing at 423 cm^{-1} is assigned to a vibration of predominant Mo–S character. Chlorine 2p photoelectron spectra were resolved into components giving binding energies for bridging, terminal, and ionic chloride in the structures. Relative areas of the component peaks confirm that sulfide must occupy a bridging ligand position in the $(Mo_6Cl_7S)^{3+}$ cluster.

Introduction

The discovery of the Chevrel phases $M_x^{n+}Mo_6X_8^{n-}$ has generated great interest among both chemists and physicists because many of these compounds are superconductors.[2] Structurally the Chevrel phases[3-7] consist of $Mo_6X_8^{n-}$ cluster units (X = chalcide) interlinked in three dimensions to form a framework in which sites are available to accommodate the ternary metal ions M^{n+}. Weak Mo–Mo bonds are formed between neighboring cluster units, and these provide the path for the conduction electrons.[2]

The Mo_6X_8 clusters of the Chevrel phases are very similar in structure to the $Mo_6X_8^{4+}$ (X = halide) clusters of the α-molybdenum(II) halides and their derivatives.[8,9] However, none of the halide clusters are interlinked in such a way that *intercluster* Mo–Mo bonds can be formed; instead, the $Mo_6X_8^{4+}$ halide clusters are well separated and behave as discrete units connected only by halide bridges in the solid state. Thus the halide cluster units are easily obtained as ligated molecular derivatives $(Mo_6X_8)L_6$. So far such discrete molecular derivatives of the Mo_6X_8 chalcide cluster units have not been prepared. The latter would be of great interest so that the bonding and properties of the chalcide cluster units could be elucidated in the absence of the strongly perturbing intercluster Mo–Mo interactions found in the Chevrel phases. Potentially an important group of compounds may exist where halogen is replaced by chalcide in steps to generate the entire series $Mo_6X_{8-x}Y_x$ (X = halide, Y = chalcide; $0 \leq x \leq 8$).

In this work the first step in the $Mo_6X_{8-x}Y_x$ substitution series has been achieved. The $(Mo_6Cl_7S)^{3+}$ cluster has been prepared and isolated in the two pyridinium salts $(C_5H_5NH)_3[(Mo_6Cl_7S)Cl_6]$ and $(C_5H_5NH)_3[(Mo_6Cl_7S)Cl_6]\cdot 3(C_5H_5NH)Cl$. The crystal and molecular structures and infrared and Cl 2p PE spectra have been determined. A comparison of these results with existing data for $Mo_6Cl_8^{4+}$ derivatives permits evaluation of the consequences of substitution of a single sulfide into the halide cluster unit.

Experimental Section

Materials. Certified ACS grade pyridine (Fisher Scientific Co.) was vacuum distilled onto outgassed 4A molecular sieves and vacuum distilled as needed. Certified ACS grade methanol (Fisher Scientific Co.) and electronic grade hydrochloric acid (Dupont) were used as received. α-Molybdenum(II) chloride was prepared according to the method of Dorman and McCarley.[10] In this procedure, molybdenum(V) chloride is reduced in an aluminum chloride rich sodium tetrachloroaluminate melt. The molybdenum(II) chloride product is extracted into an ethanol solution. Addition of hydrochloric acid and evaporation of the solution produces crystals of $(H_3O)_2[(Mo_6Cl_8)Cl_6]\cdot 6H_2O$. Heating this product in vacuo at 350 °C for 24 h yields pure, anhydrous $(Mo_6Cl_8)Cl_4$. Anhydrous sodium hydrosulfide was prepared by reaction of hydrogen sulfide with sodium ethoxide by using the procedure described by Brauer.[11] Both Mo_6Cl_{12} and NaSH were stored in a drybox (dew point ca. −75 °C).

Preparation of $(pyH)_3[(Mo_6Cl_7S)Cl_6]$. A 2.00-g (2.00-mmol) sample of Mo_6Cl_{12} and 0.22 g (3.9 mmol) of NaSH were weighed out in the drybox and transferred to a 250-mL Schlenk reflux flask equipped with a water-cooled condenser. The flask was transferred to a vacuum line (working vacuum 10^{-4}–10^{-5} torr) and outgassed, and ca. 80 mL of pyridine was distilled onto the reactants. Upon warming to room temperature, vigorous bubbling occurred, and the yellow slurry turned red. The solution was refluxed under a nitrogen atmosphere for 24 h and filtered hot under nitrogen. The pyridine was stripped from the red filtrate on the vacuum line, leaving a glassy red solid. So that the unsubstituted $Mo_6Cl_8^{4+}$ cluster could be removed, the red solid was stirred for 2 h at room temperature with ca. 35 mL of a solution of ca. 1 M HCl/CH_3OH (3 mL of concentrated HCl + 33 mL of CH_3OH). This slurry was filtered and the insoluble residue dissolved in 150 mL of hot 1 M HCl/CH_3OH. The red solution was filtered hot. Dark red crystals of product were obtained by careful evaporation of this filtrate (1.07 g, 41% yield). Anal. Calcd for $(C_5H_5NH)_3[(Mo_6Cl_7S)Cl_6]$: Mo, 43.98; Cl, 35.21; S, 2.45; C, 13.76; H, 1.39; N, 3.21; Cl/Mo, 2.17. Found: Mo, 43.50; Cl, 34.57; S, 1.84; C, 12.81; H, 1.45; N, 2.97; Cl/Mo, 2.15.

Preparation of $(pyH)_3[(Mo_6Cl_7S)Cl_6]\cdot 3pyHCl$. The reaction was similar to the one above, until the room temperature wash in HCl/CH_3OH. In the above reaction, a pale yellow solution with

---

[1] Ames Laboratory is operated for the U.S. Department of Energy by Iowa State University under Contract No. W-7405-Eng-82. This research was supported by the Assistant Secretary for Energy Research, Office of Basic Energy Sciences, Project No. WPAS-KC-02-03.

[2] Yvon, K. In "Current Topics in Materials Science", 1st ed.; Kaldis, E., Ed.; North-Holland Publishing Co.: New York, 1978; Vol. 3, Chapter 2.

[3] Bars, O.; Guillevic, J.; Grandjean, D. *J. Solid State Chem.* **1973**, *6*, 48.

[4] Guillevic, J.; Bars, O.; Grandjean, D. *J. Solid State Chem.* **1973**, *7*, 158.

[5] Marezio, M.; Dernier, P. D.; Remeika, J. P.; Corenzwit, E.; Matthias, B. T. *Mater. Res. Bull.* **1973**, *8*, 657.

[6] Chevrel, R.; Sergent, M.; Prigent, J. *Mater. Res. Bull.* **1974**, *9*, 1487.

[7] Guillevic, J.; Bars, O.; Grandjean, D. *Acta Crystallogr., Sect. B* **1976**, *B32*, 1338.

[8] Schäfer, H.; von Schnering, H. G.; Tillack, J.; Kuhnen, F. Wöhrle, H.; Baumann, H. *Z. Anorg. Allg. Chem.* **1967**, *353*, 281. Further information based on a more accurate structure refinement was kindly provided by Professor von Schnering.

[9] Guggenberger, L. J.; Sleight, A. W. *Inorg. Chem.* **1969**, *8*, 2041.

[10] Dorman, W. C.; McCarley, R. E. *Inorg. Chem.* **1974**, *13*, 491.

[11] Brauer, G. "Handbuch der Präparativen Anorganischen Chemie", 2nd ed.; Ferdinand Enke: Stuttgart, 1960; p 325.

0020-1669/82/1321-1864$01.25/0

Table I. Summary of Crystal Data, Intensity Collection, and Structure Refinement

	$(C_5H_5NH)_3[(Mo_6Cl_7S)Cl_6]\cdot 3(C_5H_5NH)Cl$	$(C_5H_5NH)_3[(Mo_6Cl_7S)Cl_6]$
formula wt	1655.61	1308.92
space group	$Pa3$	$P2_1/c$
a, Å	17.158 (2)	13.469 (4)
b, Å		15.329 (3)
c, Å		17.112 (5)
β, deg		107.19 (3)
Z	4	4
ρ_{calcd}, g cm^{-3}	2.18	2.58
ρ_{obsd}, g cm^{-3}	2.18 (flotation in 1,2-$C_2H_4Br_2$)	2.6 (flotation)
μ, cm^{-1}	23.3	32.0
no. of reflctns for detn of cell consts	12	17
λ(Mo Kα), Å	0.709 54	0.709 54
monochromator	graphite crystal	graphite crystal
takeoff angle, deg	4.5	4.5
2θ limit, deg	50	45
octants measured	h,k,l	$h,\pm k,\pm l$
no. of data, $I > 3\sigma(I)$	2558	6942
no. of unique data	816	3347
function minimized	$\Sigma w(\lvert F_o\rvert - \lvert F_c\rvert)^2$, $w = 1/\sigma_F{}^2$	$\Sigma w(\lvert F_o\rvert - \lvert F_c\rvert)^2$
R	0.054	0.063
R_w	0.058	0.074

insoluble solid resulted from this wash. If 35 mL of 2 M HCl/CH_3OH, with a few drops of added pyridine, is used for the room-temperature wash, a pale red solution (with insoluble residue) results after ca. 2$^1/_2$ h. From this solution 0.58 g of beautiful red octahedral crystals of $(pyH)_3[(Mo_6Cl_7S)Cl_6]\cdot 3pyHCl$ were isolated (18% yield). A small amount of coprecipitated $(pyH)_2[(Mo_6Cl_8)Cl_6]$ (yellow crystals) was separated from the octahedra under the microscope. The insoluble residue from the first washing in HCl/CH_3OH was dissolved in hot HCl/CH_3OH and filtered. A 0.41-g sample of $(pyH)_3[(Mo_6Cl_7S)Cl_6]$ was subsequently isolated (16% yield). Anal. Calcd for $(C_5H_5NH)_3[(Mo_6Cl_7S)Cl_6]\cdot 3(C_5H_5NHCl)$: Mo, 34.77; Cl, 34.26; S, 1.94; C, 21.76; H, 2.19; N, 5.07; Cl/Mo, 2.67. Found: Mo, 34.49; Cl, 34.32; S, 1.93; C, 21.49; H, 2.20; N, 4.98; Cl/Mo, 2.69.

Chemical Analyses. Weighed samples for molybdenum analyses were decomposed by treatment with ammonia–hydrogen peroxide solution, heated to dryness, treated with concentrated nitric acid, and again heated to dryness. This decomposition was repeated 2 or 3 times, prior to ignition of the sample to MoO_3. Solutions for chloride and sulfate analysis were prepared by decomposing weighed samples in basic aqueous solutions of sodium peroxide. The solutions were acidified, and excess H_2O_2 was expelled prior to analysis. Chloride was determined potentiometrically with a standardized silver nitrate solution. The sulfur content of $(pyH)_3[(Mo_6Cl_7S)Cl_6]$ was determined gravimetrically as $BaSO_4$. Sulfur in $(pyH)_3[(Mo_6Cl_7S)Cl_6]\cdot 3pyHCl$ was measured by Chemalytics, Inc. Carbon, hydrogen, and nitrogen was determined by the Ames Laboratory Analytical Services. Infrared spectra (4000–200 cm^{-1}) were measured as Nujol mulls between CsI plates on a Beckman IR 4250 spectrometer. Reported frequencies are considered accurate to ±2 cm^{-1}.

Chlorine 2p Photoelectron Spectra. Freshly prepared, carefully purified samples were ground in a drybox and spread onto a strip of Ag–Cd alloy and then transferred directly into the AEI ES200B spectrometer. Monochromatic Al Kα radiation (KE = 1486.6 eV) was used to irradiate the sample. The electrostatic charge which accumulated at the sample surface during irradiation was maintained at a constant equilibrium value by means of an electron flood gun, which bathed the sample in "zero volt electrons". Good signal to noise ratios resulted when data were accumulated during 400–500 scans over the range of electron binding energies of interest.

The spectral data (number of electron counts for each incremental value of the binding energy within the range recorded) were input to the APES computer program, developed in this laboratory.[12] The program corrects the data and then attempts to fit it with a linear combination of Gaussian and Lorentzian functions. The corrections include (a) two consecutive three (adjacent) point smoothings of the data, (b) a base line adjustment, so that the minimum number of counts equal zero, and (c) a correction for inelastic scattering using the method described by Shirley.[13] Next, the program calculates a fit to the corrected data, using programmer-supplied values for (a) the number of component peaks, (b) the approximate energies and heights of the component peaks, and (c) the full width at half-maximum (fwhm) of the component peaks. The energy and height of each component peak are refined by nonlinear least squares during fitting. The fwhm of each peak can also be varied. Constraints can be put on the refinement: e.g., coupling two spin–orbit coupled component peaks (Cl $2p_{1/2}$, $2p_{3/2}$) or requiring equal fwhm for all the component peaks.

The quality of the fit can be assessed from computer-generated plots of calculated and observed spectra and from χ^2. The physical reasonableness of the refined results must be judged by the programmer. In the compounds described here, the energy separation between spin–orbit coupled peaks and the fwhm of the peaks each fall within a narrow range (see Table VII). The program is particularly helpful if the programmer has a limited number of possible model structures for the compound. Then it can be used to refine the heights of the component peaks in fixed ratios corresponding to the relative ratios of nonequivalent chlorides in the model. The best model corresponds to the best fit.

X-ray Structure Determinations

Collection and Reduction of X-ray Data for $(pyH)_3[(Mo_6Cl_7S)Cl_6]\cdot 3pyHCl$. This compound crystallizes as beautiful red octahedra. The length of the apparent 3-fold axes of the selected crystal was 0.019 cm. All corners of the octahedron were slightly truncated. The crystal was mounted with a 3-fold axis approximately collinear with ϕ on an automated four-circle diffractometer.[14] Eight reflections were selected from ω-oscillation photographs taken at ϕ = 0, 30, 60, and 90°. The angular coordinates of the eight reflections were input to the automatic indexing program ALICE,[15] which calculated the orientation matrix, the reduced unit cell, and the reduced cell scalars. These approximate cell parameters and the scalars indicated cubic crystal symmetry.

The method of data collection has been described.[14] Accurate unit cell parameters and their estimated standard deviations given in Table I were determined by a least-squares fit to the $\pm 2\theta$ values of 12 independent high-angle ($2\theta \geq 30°$) reflections. The intensity data were then corrected for Lorentz–polarization effects. An absorption correction was not necessary. Weakly observed reflections were discarded if less than half of their symmetry-related reflections were observed. The remaining equivalent data were averaged and used in the structure refinement, as indicated in Table I.

Solution and Refinement of the Structure. A total of 816 independent reflections were used in the structure refinement. The $0kl$ reflections with $l = 2n + 1$ were systematically unobserved. In order

---

(12) Luly, M. H. "APES, A Fortran Program to Analyze Photoelectron Spectra", US DOE Report IS-4694; Iowa State University: Ames, IA, 1979.

(13) Shirley, D. A. *Phys. Rev. B* **1972**, *5*, 4709.

(14) Rohrbaugh, W. J.; Jacobson, R. A. *Inorg. Chem.* **1974**, *13*, 2535.

(15) Jacobson, R. A. *J. Appl. Crystallogr.* **1976**, *9*, 115.

Table II. Final Positional Parameters for $(C_5H_5NH)_3[(Mo_6Cl_7S)Cl_6]\cdot 3(C_5H_5NH)Cl$[a]

atom	x	y	z
Mo	0.47921 (6)	0.52633 (6)	0.60219 (6)
X(1)	0.6019 (5)	0.6019 (5)	0.6019 (5)
X(2)	0.5518 (2)	0.4082 (2)	0.6415 (2)
Cl	0.4535 (2)	0.5615 (2)	0.7386 (2)
Cl,i	0.1923 (8)	0.1923 (8)	0.1923 (8)
Cl,is	0	0	0
R(1)	0.186 (2)	0.246 (2)	0.877 (1)
R(2)	0.235 (1)	0.244 (1)	0.932 (2)
R(3)	0.230 (1)	0.192 (2)	0.992 (1)
R(4)	0.174 (2)	0.138 (1)	0.989 (2)
R(5)	0.123 (1)	0.140 (1)	0.932 (3)
R(6)	0.130 (2)	0.196 (2)	0.874 (2)
H(1)	0.19	0.29	0.83
H(2)	0.29	0.29	0.94
H(3)	0.27	0.19	1.04
H(4)	0.17	0.09	1.04
H(5)	0.08	0.10	0.93
H(6)	0.09	0.19	0.83

[a] Numbers in parentheses are the estimated standard deviations of the coordinates and refer to the last significant digit of the preceding number.

that the structure could be refined in the space group *Pa*3, the *k* and *l* indices of all reflections were interchanged and the signs of the new *k* indices changed.

The position of the molybdenum atom was located with Patterson superposition techniques.[16] The bridging ligand, ionic, and terminal chloride positions were determined from subsequent electron density maps.[17] (Note: Because of the very similar X-ray scattering power of Cl and S, we were unable to ascertain whether S is localized on one of the two independent sets of bridging ligand sites of the $Mo_6Cl_7S^{3+}$ cluster or disordered over both. The scattering factor of Cl was used in the refinement of both sets of bridging ligand parameters.) Following refinement of the positional and isotropic thermal parameters of these atoms, the discrepancy factor ($R = \sum||F_o| - |F_c||/\sum|F_o|$) was 0.189. The six atom positions defining the pyridinium cation were determined from sharpened electron density difference maps.[18] Because these six positions could not be distinguished, they were refined with an averaged scattering factor (${}^1/_6$ N, ${}^5/_6$ C). At this point, problems were encountered in the refinement of all 12 atoms due to severe overshifting of the constrained X(1) and Cl, i positional parameters (both on c sites with 3 site symmetry). The refinement of these positions, and subsequently of the anistropic thermal parameters of these atoms and of Cl,is (a site, $\bar{3}$ site symmetry) was damped by using half shifts. Prior to anisotropic refinemenmt of the pyridinium cation, its hydrogen atom positions were calculated and input but not refined. The positions and anisotropic thermal parameters of all nonhydrogen atoms were refined by full-matrix least-squares techniques,[18] with use of the scattering factors of Hanson et al.,[19] with molybdenum and chlorine corrected for the real and imaginary parts of anomalous dispersion.[20] There was no significant electron density (>1 e/Å^3) in the final electron density difference map. Final parameters are listed in Table II.

Collection and Reduction of X-ray Data for $(pyH)_3[(Mo_6Cl_7S)Cl_6]$. This compound crystallizes in the form of dark red cubes. A number of these crystals were checked, and all were twinned. An irregularly shaped crystal chip (not a twin) of dimensions 0.026 × 0.017 × 0.010 cm was chosen for the structure determination. Crystal indexing indicated a monoclinic unit cell. Data collection proceeded as before.[14] Since a slight decrease in the standards' intensities occurred, a scaling procedure was used to normalize the raw data. The intensity data were corrected for Lorentz–polarization effects. Although several attempts were made to correct the data for absorption with the Tompa–Alcock program, none of the corrected data sets refined as well as the uncorrected one. Calculated transmission factors ranged from 0.68 to 0.83. Equivalent reflections were averaged; the criterion for inclusion in the data set was $(|F_o| - |F_a|)/|F_a| \le 0.20$. Other pertinent information is included in Table I.

Table III. Final Positional Parameters for $(C_5H_5NH)_3[(Mo_6Cl_7S)Cl_6]$[a]

atom	x	y	z
Mo(1c)	0.87359 (9)	0.94560 (8)	0.48487 (8)
Mo(2c)	1.04372 (9)	0.95781 (8)	0.60558 (7)
Mo(3c)	0.94890 (9)	1.09809 (8)	0.53659 (7)
Mo(1b)	0.52761 (9)	0.39983 (8)	0.45126 (7)
Mo(2b)	0.53451 (9)	0.44436 (8)	0.59942 (7)
Mo(3b)	0.36381 (9)	0.46521 (8)	0.48109 (7)
X(1c)	0.8735 (3)	0.0018 (3)	0.6190 (2)
X(2c)	0.9700 (3)	0.8147 (2)	0.5505 (2)
X(3c)	0.1138 (3)	0.1042 (2)	0.6505 (2)
X(4c)	0.7895 (3)	1.0818 (2)	0.4198 (2)
X(1b)	0.4295 (3)	0.3188 (2)	0.5302 (2)
X(2b)	0.6884 (3)	0.3849 (2)	0.5664 (2)
X(3b)	0.3783 (3)	0.5098 (3)	0.6220 (2)
X(4b)	0.3640 (3)	0.4255 (2)	0.3399 (2)
Cl(1c)	0.7062 (3)	0.8730 (3)	0.4660 (3)
Cl(2c)	1.0999 (3)	0.9049 (3)	0.7470 (2)
Cl(3c)	0.8811 (3)	1.2293 (3)	0.5848 (3)
Cl(1b)	0.5637 (4)	0.2619 (3)	0.3912 (3)
Cl(2b)	0.5809 (3)	0.3675 (3)	0.7308 (2)
Cl(3b)	0.1837 (3)	0.4155 (3)	0.4570 (3)
N(1)	0.531 (2)	0.386 (2)	0.183 (1)
C(1)	0.589 (2)	0.337 (2)	0.149 (2)
C(2)	0.626 (2)	0.386 (2)	0.091 (2)
C(3)	0.608 (2)	0.479 (2)	0.082 (2)
C(4)	0.541 (3)	0.521 (2)	0.124 (2)
C(5)	0.509 (2)	0.474 (2)	0.171 (2)
N(2)	0.202 (2)	0.716 (2)	0.688 (1)
C(6)	0.122 (2)	0.672 (2)	0.725 (2)
C(7)	0.066 (2)	0.598 (2)	0.682 (2)
C(8)	0.085 (2)	0.574 (2)	0.613 (2)
C(9)	0.149 (2)	0.616 (2)	0.579 (2)
C(10)	0.202 (2)	0.681 (2)	0.616 (2)
N(3)	0.885 (2)	0.820 (1)	0.770 (1)
C(11)	0.806 (2)	0.800 (2)	0.695 (2)
C(12)	0.707 (2)	0.792 (2)	0.704 (2)
C(13)	0.689 (2)	0.800 (2)	0.775 (1)
C(14)	0.768 (2)	0.818 (2)	0.844 (1)
C(15)	0.867 (2)	0.831 (2)	0.840 (2)

[a] Numbers in parentheses are the estimated standard deviations of the coordinates and refer to the last significant digit of the preceding number.

Solution and Refinement of the Structure. A total of 3347 independent reflections were used in the structure refinement. The $h0l$ with $l = 2n + 1$ and $0k0$ with $k = 2n + 1$ reflections were systematically absent, indicating the $P2_1/c$ space group. The molybdenum and bridging and terminal ligand positions were located as before. (Note: Because we were also unable to ascertain the disposition of S over the bridging ligand sites of this $(Mo_6Cl_7S)^{3+}$ cluster, the bridging ligand parameters were again refined with the scattering factor of chlorine.) Refinement of the positions and isotropic thermal parameters of these atoms resulted in a discrepancy factor of 0.149. The carbon and nitrogen positions of the pyridinium cations were located in sharpened electron density difference maps.[18] Because the distinction between N and C atoms was not checked during final stages of the structure refinement (as it was in the case of $(pyH)_3[(Mo_6Cl_7S)Cl_6]\cdot 3pyHCl$), this distinction is tentative; i.e., the nitrogen may again be disordered over all six sites of each ring. Subsequent refinement proceeded smoothly. All atoms except for carbon and nitrogen were refined anisotropically by full-matrix least-squares techniques.[18] Because of the large thermal parameters of the carbon and nitrogen atoms, they were refined isotropically. There was no significant electron density in the final electron density difference map.[17] Final positional parameters are listed in Table III. Tables of observed and

---

(16) Hubbard, C. R.; Babich, M. W.; Jacobson, R. A. "A PL/1 Program System for Generalized Patterson Superpositions", US AEC Report IS-4106; Iowa State University: Ames, IA, 1977.

(17) Hubbard, C. R.; Quicksall, C. O.; Jacobson, R. A. "The Fast Fourier Algorithm and the Programs ALFF, ALFFDP, ALFFPROJ, ALFFT, and Friedel", US AEC Report IS-2625; Iowa State University: Ames, IA, 1971.

(18) Lapp, R. L.; Jacobson, R. A. "ALLS, A Generalized Crystallographic Least Squares Program", US DOE Report IS-4708; Iowa State University: Ames, IA, 1979.

(19) Hanson, H. P.; Herman, F.; Lea, J. D.; Skillman, S. *Acta Crystallogr.* **1964**, *17*, 1040.

(20) Templeton, D. H. In "International Tables for X-ray Crystallography", 1st ed.; Macgillavry, C. H., Rieck, G. D., Eds.; Kynoch Press: Birmingham, England, 1962; Vol. III, p 215.

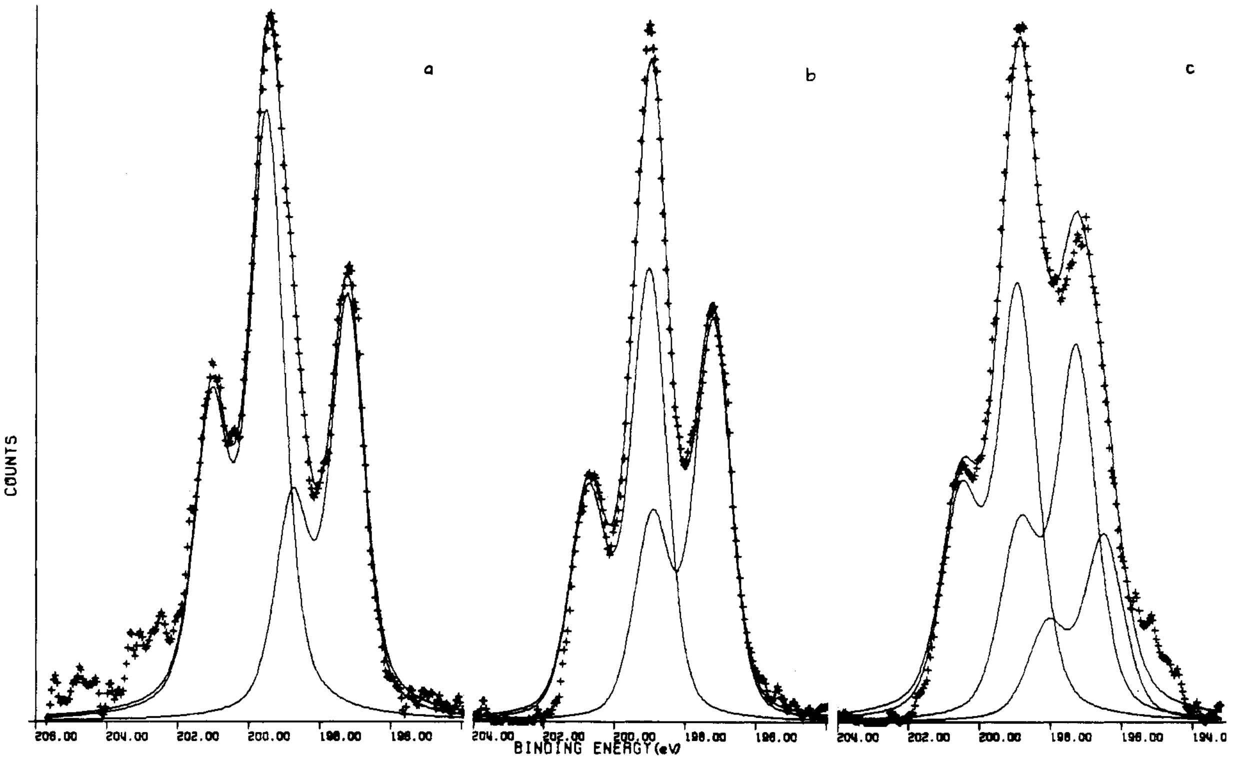

Figure 1. Chlorine 2p photoelectron spectra of $[(n\text{-}C_4H_9)_4N]_2[(Mo_6Cl_8)Cl_6]$ (a), $(C_5H_5NH)_3[(Mo_6Cl_7S)Cl_6]$ (b), and $(C_5H_5NH)_3[(Mo_6Cl_7S)Cl_6]\cdot 3(C_5H_5NH)Cl$ (c). The + marks indicate smoothed and treated data points. The solid line through the points represents the best least-squares fit to the data and the sum of the component peaks (lower curves) shown in the figure.

calculated structure factors and anisotropic thermal parameters are available as supplementary material.

Results and Discussion

Syntheses. The chemistry of α-molybdenum(II) chloride and its derivatives is straightforward in view of the structure of these compounds.[8,9] (Note: The structure of a $(Mo_6Cl_8)L_6$ cluster is identical with that of the $(Mo_6Cl_7S)Cl_6^{3-}$ cluster, shown in Figure 1.) The cornerstone of the structure is the $Mo_6Cl_8^{4+}$ unit, which consists of an octahedron of bonded molybdenum atoms, with a "bridging" chloride capping each face of the octahedron. The eight bridging chlorides define the vertices of a cube, with a molybdenum atom near the center of each cube face. Each molybdenum atom has a coordination site, located on the normal to its face of the cube; the six coordination sites of this type are occupied by "terminal" ligands.

Because of the cluster's strongly bonded framework, it can undergo ligand substitution without decomposition. The terminal ligands are relatively labile.[21-26] However, since each bridging chloride forms three strong Mo–Cl bonds, substitution at these sites of the $Mo_6Cl_8^{4+}$ cluster requires vigorous reaction conditions or nucleophiles. If the attacking ligand is bromide or iodide, complete substitution proceeds smoothly in the lithium halide melt, yielding the stable $Mo_6X_8^{4+}$ (X = Br, I) clusters.[27] However, substitution by nonhalides frequently causes cluster decomposition due to the instability of the desired products toward degradative oxidation. No more than two hydroxides can be substituted into the bridging chloride sites of $Mo_6Cl_8^{4+}$ before cluster degradation occurs.[26,28] The cluster is more tolerant toward substitution by methoxide. Complete substitution is possible, but the resulting compound, $Na_2[(Mo_6(OCH_3)_8)(OCH_3)_6]$, is pyrophoric.[29]

The results given here demonstrate that substitution by sulfide occurs under relatively mild conditions and yields stable products. In the first step of the synthesis of $(Mo_6Cl_7S)Cl_6^{3-}$, α-molybdenum(II) chloride is reacted with sodium hydrosulfide in pyridine. Dissolution of the amorphous Mo_6Cl_{12} causes vigorous bubbling. Before the slurry reaches reflux temperature, a flocculent, brilliant red precipitate forms. If this intermediate is isolated and reacted with HCl/CH_3OH, it yields $(pyH)_2[(Mo_6Cl_8)Cl_6]$, strong evidence that the red intermediate contains an untouched $Mo_6Cl_8^{4+}$ cluster, with sulfide in some of the terminal ligand sites. Substitution of sulfide into a bridging site is achieved more slowly by refluxing the reaction mixture for 24 h. After NaCl and other insoluble byproducts are filtered off, the solvent is stripped from the filtrate on a vacuum line, yielding a glassy red product. The infrared spectrum of the product consists of bands assigned either to vibrations of coordinated pyridine[30] or to Mo–Cl vibrations.[31] The product is formulated as $(Mo_6Cl_7S)Cl_3(C_5H_5N)_3$ on the basis of characterization of its hydrochlorinated derivative.

Thus, the overall reaction in pyridine is

$$Mo_6Cl_{12} + 2NaSH \xrightarrow{py} (Mo_6Cl_7S)Cl_3(py)_3 + 2NaCl + (pyH)SH$$

Subsequent reaction with HCl yields the final product:

$$\text{“}(Mo_6Cl_7S)Cl_3(py)_3\text{”} + 3HCl \rightarrow (pyH)_3[(Mo_6Cl_7S)Cl_6]$$

Depending on the concentrations of Cl^- and pyH^+ in the so-

---

(21) Cotton, F. A.; Curtis, N. F. *Inorg. Chem.* **1965**, *4*, 241.
(22) Sheldon, J. C. *J. Chem. Soc.* **1960**, 1007.
(23) Schäfer, H.; Plautz, H. *Z. Anorg. Allg. Chem.* **1972**, *389*, 57.
(24) Lessmeister, P.; Schäfer, H. *Z. Anorg. Allg. Chem.* **1975**, *417*, 171.
(25) Weissenhorn, R. G. *Z. Anorg. Allg. Chem.* **1976**, *426*, 159.
(26) Baumann, H.; Plautz, H.; Schäfer, H. *J. Less-Common Met.* **1971**, *24*, 301.
(27) Sheldon, J. C. *J. Chem. Soc.* **1962**, 410.
(28) Sheldon, J. C. *Chem. Ind. (London)* **1961**, 323.
(29) Nannelli, P.; Block, B. P. *Inorg. Chem.* **1968**, *7*, 2423.
(30) Gill, N. S.; Nattall, R. H.; Scaife, D. E.; Sharp, D. W. A. *J. Inorg. Nucl. Chem.* **1961**, *18*, 79.
(31) Mackay, R. A. Ph.D. Dissertation, State University of New York at Stony Brook, 1966.

Table IV. Low-Frequency Infrared Data (200-450 cm^{-1})[a]

$(C_5H_5NH)_3[(Mo_6Cl_7S)Cl_6]$	$(C_5H_5NH)_3[(Mo_6Cl_7S)Cl_6]\cdot 3(C_5H_5NH)Cl$	$[(n\text{-}C_4H_9)_4N]_2[(Mo_6Cl_8)Cl_6]$	$(C_5H_5NH)_2[(Mo_6Cl_8)Cl_6]$
421 ms	423 m		
389 w	390 m	388 vw	390 vw
		376 vw	
362 w		355 sh	355 w, sh
	344 w		
312 vs	310 vs	325 vs	321 vs
	271 vw, sh	271 vw, sh	266 vw
230 s	230 ms	237 s	236 vs
218 sh	213 sh	214 w m	209 m

[a] Spectra obtained from Nujol mulls. Abbreviations: s, strong; m, medium; w, weak; v, very; sh, shoulder.

lution, this salt is isolated neat or is isolated with three formula units of pyHCl in the lattice as $(pyH)_3[(Mo_6Cl_7S)Cl_6]\cdot 3pyHCl$. Crystals of both salts of the $(Mo_6Cl_7S)Cl_6^{3-}$ anion are indefinitely stable in air; solutions in acetonitrile or CH_3OH/HCl are slowly (weeks) oxidized.

Increasing the proportion of NaSH in the reaction yields more extensively substituted products. Crystalline products with five to six bridging sulfides per cluster, isolated from the reaction in pyridine, will be the subject of subsequent publications.

Spectroscopic Characterization. The physical techniques used to characterize these two compounds provide essential data in the determination of their structures and compositions. The X-ray structure determinations indicated the structures of the two formula units $(pyH)_3[(Mo_6X_8)X_6]$ and $(pyH)_3[(Mo_6X_8)X_6]\cdot 3pyHCl$. The analytical data agree quite well with the respective formulations $(pyH)_3(Mo_6Cl_{13}S)$ and $(pyH)_6(Mo_6Cl_{16}S)$. At this stage, despite chemical evidence indicating sulfide occupied a bridging ligand site (i.e., reaction with HCl did not regenerate $(Mo_6Cl_8)Cl_6^{2-}$), the question of whether sulfide occupied a bridging or terminal ligand site was still moot. The chlorine 2p photoelectron spectra indicate *unambiguously* that the sulfide in both compounds is in bridging ligand site; thus, the two compounds are $(pyH)_3[(Mo_6Cl_7S)Cl_6]$ and $(pyH)_3[(Mo_6Cl_7S)Cl_6]\cdot 3pyHCl$. The infrared spectra of both compounds agree closely in the 200-450-cm^{-1} region, good evidence that $(Mo_6Cl_7S)Cl_6^{3-}$ is the cluster species in both compounds.

Finally, there is little question that the sulfides are deprotonated after insertion into the cluster. A triply bridging SH^- ligand is unknown, presumably because it is quite acidic. The absence of an electron spin resonance signal for either compound leaves very little doubt; if the sulfide were protonated, both compounds would have an odd number of electrons.

Infrared Spectra. The infrared spectra of the two compounds are practically identical; some bands assigned to the pyridinium cation[30] are more intense in the spectrum of $(pyH)_3[(Mo_6Cl_7S)Cl_6]\cdot 3pyHCl$. The equivalence of the spectra in the Mo-Cl stretching region confirms that the same $(Mo_6Cl_7S)Cl_6^{3-}$ unit is present in both compounds. Predictably, the pattern of the bands in this region is quite similar to that of $(Mo_6Cl_8)Cl_6^{2-}$. However, inspection of Table IV demonstrates that band locations and intensities in the spectra of the $(Mo_6Cl_7S)Cl_6^{3-}$ and $(Mo_6Cl_8)Cl_6^{2-}$ clusters are significantly different. Also, a new band appears in the spectrum of $(Mo_6Cl_7S)Cl_6^{3-}$ at 421 cm^{-1}. This band has not been observed in the spectra of other pyridinium salts, and its frequency is too high for a Mo^{II}-Cl vibration of a hexanuclear cluster.[31] Thus, this band is unique to the $(Mo_6Cl_7S)Cl_6^{3-}$ cluster unit. Caution must be exercised in assigning this band since Hogue and McCarley have shown that extensive mixing of the normal vibrational modes of M_6X_8 clusters occurs.[32] Thus, although the normal mode giving rise to the 421-cm^{-1} band undoubtedly mixes with the other modes of the $(Mo_6Cl_7S)Cl_6^{3-}$ cluster, it can be assigned to a vibration of *predominant* Mo-S character. The high frequency of this vibration is not unreasonable when compared to the Mo_3S vibration at 459 cm^{-1} of the $[Mo_3(\mu_3\text{-}S)(\mu_2\text{-}S_2)_3(S_2)_3]^{2-}$ cluster anion.[33]

Chlorine 2p Photoelectron Spectra. X-ray photoelectron spectroscopy (PES) has been developed into an important tool for the structural characterization of transition-metal halides.[34,35] Because the binding energy of the core level electrons of an atom are sensitive to its chemical environment, PES can be used to determine the number of different "types" of halide (triply bridging, terminal, etc.) in a metal halide. Hamer and Walton[36] have demonstrated that α-molybdenum(II) chloride an its derivatives are a particularly favorable case because of a large binding energy difference between the triply bridging and terminal chlorides in these compounds of ca. 2.3 eV. Thus, although the Cl 2p photoelectron spectra are complicated by spin-orbit coupling (each type of chloride has two spin-orbit coupled peaks, with a binding energy separation of ca. 1.5 eV), the spectra of these compounds can be resolved into component peaks and the ratio of the number of bridging to the number of terminal chlorides (Cl_b/Cl_t) estimated.

The calculated and observed Cl 2p photoelectron spectra of three compounds are shown in Figure 1. An excellent fit was achieved for the spectrum of $[(n\text{-}C_4H_9)_4N]_2[(Mo_6Cl_8)Cl_6]$, with a ratio of $Cl_b/Cl_t = 1.43$ ($^8/_6 = 1.33$ is the correct value). An excellent fit was also obtained for the Cl 2p spectrum of $(pyH)_3[(Mo_6Cl_7S)Cl_6]$, with a ratio $Cl_b/Cl_t = 1.12$. Any remaining ambiguity in the location of sulfide in the $Mo_6Cl_{13}S^{3-}$ anion is dispelled; of the two possible models, $(Mo_6Cl_7S)Cl_6^{3-}$ (expected ratio $Cl_b/Cl_t = 1.17$) and $(Mo_6Cl_8)SCl_5^{3-}$ (expected ratio $Cl_b/Cl_t = 1.60$), the first is obviously the correct one. Prior to the solution of the X-ray crystal structure of $(pyH)_3[(Mo_6Cl_7S)Cl_6]\cdot 3pyHCl$, we determined that this compound probably had three types of chloride because we were unable to fit the observed Cl 2p photoelectron spectrum with only two types. The calculated spectrum shown in Figure 1 was obtained by fixing the ratio $Cl_b/Cl_t/Cl_i$ at the correct value (7/6/3). A better fit was obtained without this constraint but was not physically reasonable. Of the reasonable models, this correct model gave the best fit.

Table V lists data derived from these calculated spectra, along with corresponding data for two other salts of $[(Mo_6Cl_8)Cl_6]^{2-}$. Although reference to the C 1s spectrum was used to determine the binding energies in these two $(Mo_6Cl_8)Cl_6^{2-}$ salts, corresponding binding energies differ by 0.4-0.5 eV. However, the difference in binding energy between the bridging and terminal chlorides (the binding energy "shift")

---

(32) Hogue, R. D.; McCarley, R. E. *Inorg. Chem.* **1970**, *9*, 1354.

(33) Müller, A.; Sarkar, S.; Bhattacharyya, R. G.; Pohl, S.; Dartmann, M. *Angew. Chem.* **1978**, *90*, 564.

(34) Walton, R. A. *Coord. Chem. Rev.* **1976**, *21* 63.

(35) Walton, R. A. *J. Less-Common Met.* **1977**, *54*, 71.

(36) Hamer, A. D.; Walton, R. A. *Inorg. Chem.* **1974**, *13*, 1446.

Table V. Chlorine 2p Photoelectron Data

compd	Cl $2p_{3/2}$ BE,[a] eV bridging	terminal	ionic	fwhm,[b] eV	ESSO,[b] eV	ref
$((n\text{-}C_4H_9)_4N)_2[(Mo_6Cl_8)Cl_6]$	199.4	197.2		1.14	1.55	this work
$(C_5H_5NH)_3[(Mo_6Cl_7S)Cl_6]$	199.0	197.2		1.20	1.70	this work
$(C_5H_5NH)_3[(Mo_6Cl_7S)Cl_6]\cdot 3(C_5H_5NH)Cl$	198.9	197.2	196.4	1.30	1.60	this work
$((C_2H_5)_4N)_2[(Mo_6Cl_8)Cl_6]$[c]	200.1	197.8			1.6, 1.6	36
$(H_3O)_2[(Mo_6Cl_8)Cl_6]$[c]	199.6	197.4			1.6, 1.4	36

[a] Unless noted otherwise, the reference for all binding energy (BE) data is the C 1s binding energy (284.0 eV) of the cation. [b] Abbreviations: fwhm, full-width at half-maximum of resolved component; ESSO, energy separation between spin-orbit coupled peaks. [c] Reference is C 1s binding energy (284.0 eV) of graphite contaminant.

is nearly identical in all three $(Mo_6Cl_8)Cl_6^{2-}$ salts. Thus, although comparison of corresponding binding energies in a series of compounds is risky, comparisons of binding energy shifts are quite valid.

Corresponding Cl 2p binding energies of the two $(Mo_6Cl_7S)Cl_6^{3-}$ salts agree within 0.1 eV. Surprisingly, the binding energy shift between bridging and terminal chlorides in the $(Mo_6Cl_7S)Cl_6^{3-}$ cluster has dropped to 1.7–1.8 eV, 0.5 eV smaller than the shift observed in the isostructural, isoelectronic $(Mo_6Cl_8)Cl_6^{2-}$ cluster or any of the other derivatives of α-molybdenum(II) chloride.[36] The shift in $(Mo_6Cl_7S)Cl_6^{3-}$ is quite comparable to the binding energy shift of 1.8–1.9 eV between *doubly* bridging and terminal chlorides of $(Nb_6Cl_{12})Cl_2L_4$ (L = $(CH_3)_2SO$, $P(n\text{-}C_3H_7)_3$), and $[(C_2H_5)_4N]_3[(Nb_6Cl_{12})Cl_6]$.[37] No reason for the anomalously small shift in $(Mo_6Cl_7S)Cl_6^{3-}$ can be found in its structure; indeed, the bond distances (vide infra) indicate the bridging chlorides are bound as strongly as in α-molybdenum(II) chloride, the terminal ligands not as strongly bound, leading one to expect a slightly larger shift in $(Mo_6Cl_7S)Cl_6^{3-}$. An explanation of the anomalous binding energy shift of $(Mo_6Cl_7S)Cl_6^{3-}$ will be deferred until a definite trend can be established from the data of other sulfur-substituted clusters.

The binding energy shift between the terminal and ionic chlorides of $(pyH)_3[(Mo_6Cl_7S)Cl_6]\cdot 3pyHCl$ is 0.8 eV, halfway between the 1.6 eV Cl_t–Cl_i shifts in octahedral $(ML_2Cl_2)Cl$ complexes (M = Cr(III), Rh(III); L = 2,2′-bipyridine, 2,5-dithiahexane, 1,2-bis(diphenylphosphino)ethane, 1,2-bis(diphenylarsino)ethane) and the 0-eV shift in the analogous amine (L = NH_3, ethylenediamine) complexes.[38] Ebner et al. speculated that the binding energy of the ionic chloride in the amine $(ML_2Cl_2)Cl$ complexes had been increased by N–H---Cl hydrogen-bonding interactions, causing a decreased shift. Hydrogen bonding between the pyridinium cations and ionic chlorides of $(pyH)_3[(Mo_6Cl_7S)Cl_6]\cdot 3pyHCl$ may have a similar but apparently smaller effect. On the other hand, the intermediate value of the Cl_t–Cl_i shift of $(pyH)_3[(Mo_6Cl_7S)Cl_6]\cdot 3pyHCl$ may reflect weaker metal–Cl_t bonding in the cluster than in the monomeric complexes. However, the metal–Cl_t bond strengths in the cluster and in the complexes are not readily compared due to the dissimilarity of these two types of compounds.

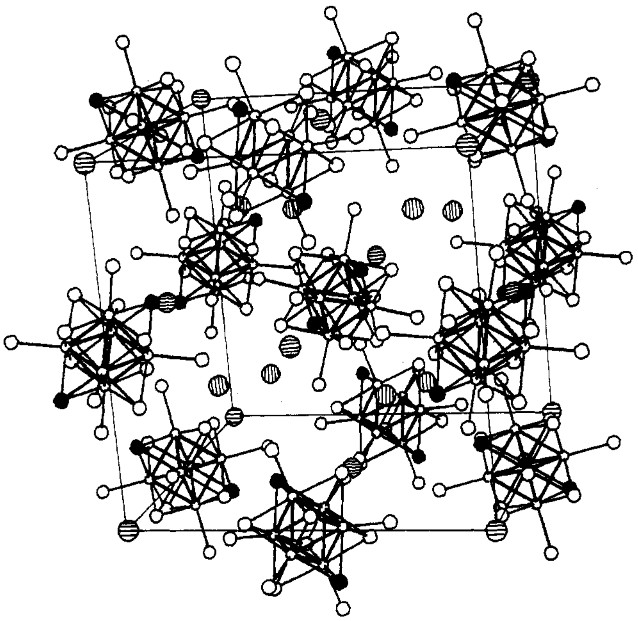

Figure 2. Perspective view of the $(Mo_6Cl_7S)Cl_6^{3-}$ clusters and chloride ions in the unit cell of $(C_5H_5NH)_3[(Mo_6Cl_7S)Cl_6]\cdot 3(C_5H_5NH)Cl$: small open circle, molybdenum; large open circle, bridging and terminal chlorides; closed circle, bridging chlorides on 3-fold; horizontally hatched circle, ionic chlorides Cl,is; vertically hatched circle, ionic chlorides Cl,i.

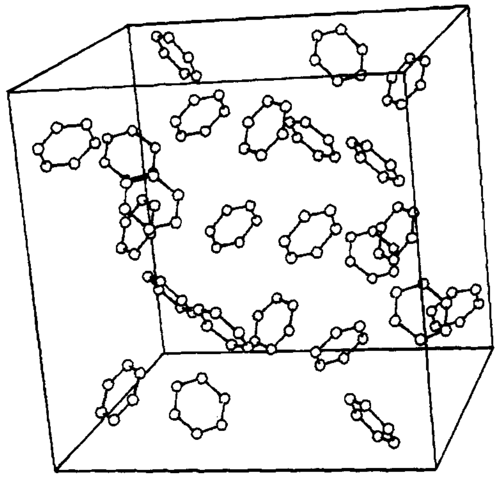

Figure 3. Perspective view of the pyridinium cations in the unit cell of $(C_5H_5NH)_3[(Mo_6Cl_7S)Cl_6]\cdot 3(C_5H_5NH)Cl$. (Note: The nitrogen atom is apparently disordered over the ring.)

X-ray Structure Determinations. The structure of $(pyH)_3[(Mo_6Cl_7S)Cl_6]\cdot 3pyHCl$ consists of $(Mo_6Cl_7S)Cl_6^{3-}$ clusters located halfway along the edges and at the body center of the cubic unit cell (b site, $\bar{3}$ site symmetry), chloride ions (Cl,is) at the origin and face centers of the unit cell (b site, $\bar{3}$ site symmetry), 8 more chloride ions (Cl,i) within the unit cell (c site, 3 site symmetry), and 24 pyridinium cations in general cell positions. For clarity, separate views of the chloride ions and clusters (Figure 2) and of the pyridinium cations (Figure 3) are presented.[39] The nearest neighbors of both types of unbound chloride ions are the pyridinium cations. There are three (Cl,i)–R1 contacts of 3.35 (3) Å, and six (Cl,is)–R5 contacts of 3.40 (3) Å. (Note: Since the six

---

(37) Best, S. A.; Walton, R. A. *Inorg. Chem.* **1979**, *18*, 484.

(38) Ebner, J. R.; McFadden, D. L.; Tyler, D. R.; Walton, R. A. *Inorg. Chem.* **1976**, *15*, 3014.

(39) Johnson, C. K. "ORTEP, A Fortran Thermal-Ellipsoid Plot Program for Crystal Structure Illustrations", US AEC Report ORNL-3794; Oak Ridge National Laboratory: Oak Ridge, TN, 1965.

Table VI. Bond Distances (Å), Nonbonded Distances (Å), and Angles (Deg) in the $(Mo_6Cl_7S)Cl_6^{3-}$ Cluster of $(C_5H_5NH)_3[(Mo_6Cl_7S)Cl_6]\cdot 3(C_5H_5NH)Cl$[a]

	Bond Distances		
Mo(1)-Mo(2)	2.608 (2)	X(2)-Mo(1)	2.473 (3)
Mo(1)-Mo(2′)	2.612 (2)	X(2)-Mo(2)	2.477 (3)
av Mo-Mo	2.610	X(2)-Mo(3′)	2.474 (3)
Cl(1)-Mo(1)	2.456 (3)	av X(2)-Mo	2.475
		X(1)-Mo(1)	2.473 (5)
		av X-Mo	2.475
	Nonbonded Distances		
X(2)-X(1)	3.499 (6)	av X-X	3.495
X(2)-X(3′)	3.493 (5)		
	Angles		
Mo(2)-Mo(1)-Mo(3)	60.00	Mo(1)-X(1)-Mo(2)	63.7 (1)
Mo(2)-Mo(1)-Mo(3′)	60.05 (3)	Mo(1)-X(2)-Mo(2)	63.59 (9)
Mo(2′)-Mo(1)-Mo(3)	60.05 (3)	Mo(1)-X(2)-Mo(3′)	63.74 (9)
Mo(2′)-Mo(1)-Mo(3′)	59.89 (5)	Mo(2)-X(2)-Mo(3′)	63.69 (8)
av Mo-Mo-Mo	60.00	av Mo-X-Mo	63.7
X(1)-Mo(1)-X(4)	90.0 (1)	X(1)-Mo(1)-Cl(1)	91.5 (1)
X(1)-Mo(1)-X(2)	90.1 (1)	X(2)-Mo(1)-Cl(1)	91.8 (1)
X(2)-Mo(1)-X(3′)	89.83 (8)	X(3′)-Mo(1)-Cl(1)	93.0 (1)
X(3′)-Mo(1)-X(4)	89.75 (9)	X(4)-Mo(1)-Cl(1)	92.7 (1)
av X-Mo-X	89.8	av X-Mo-Cl	92.3

[a] X(1), X(1′) occupy crystallographic special positions on the cluster's 3-fold axis; the other six bridging ligands are all equivalent as are all six Mo, and all six Cl atoms.

Table VII. Bond Distances (Å) and Nonbonded Distances (Å) in the $(Mo_6Cl_7S)Cl_6^{3-}$ Cluster of $(C_5H_5NH)_3[(Mo_6Cl_7S)Cl_6]$

	c sites	b sites
	Bond Distances	
Mo(1)-Mo(2)	2.599 (2)	2.601 (2)
Mo(1)-Mo(3)	2.597 (1)	2.607 (2)
Mo(1)-Mo(2′)	2.617 (2)	2.594 (2)
Mo(1)-Mo(3′)	2.611 (2)	2.600 (2)
Mo(2)-Mo(3)	2.600 (1)	2.596 (2)
Mo(2)-Mo(3′)	2.609 (2)	2.610 (2)
av Mo-Mo	2.606	2.601
Mo(1)-Mo(1′)	3.688 (2)	3.674 (2)
Mo(2)-Mo(2′)	3.688 (3)	3.672 (2)
Mo(3)-Mo(3′)	3.678 (2)	3.690 (2)
X(1)-Mo(1)	2.451 (4)	2.484 (4)
X(1)-Mo(2)	2.464 (4)	2.473 (4)
X(1)-Mo(3)	2.458 (4)	2.467 (4)
av X(1)-Mo	2.458	2.475
X(2)-Mo(1)	2.473 (4)	2.471 (4)
X(2)-Mo(2)	2.477 (4)	2.478 (4)
X(2)-Mo(3′)	2.483 (4)	2.470 (4)
av X(2)-Mo	2.478	2.473
X(3)-Mo(1′)	2.492 (4)	2.456 (4)
X(3)-Mo(2)	2.468 (4)	2.462 (4)
X(3)-Mo(3)	2.487 (4)	2.458 (4)
av X(3)-Mo	2.482	2.459
X(4)-Mo(1)	2.478 (3)	2.482 (4)
X(4)-Mo(2′)	2.486 (4)	2.467 (4)
X(4)-Mo(3)	2.476 (4)	2.492 (4)
av X(4)-Mo	2.480	2.480
av X-Mo	2.474	2.472
Mo(1)-Cl(1)	2.449 (4)	2.461 (4)
Mo(2)-Cl(2)	2.451 (4)	2.450 (4)
Mo(3)-Cl(3)	2.451 (3)	2.459 (4)
	Nonbonded Distances	
X(1)-X(2)	3.491 (6)	3.506 (5)
X(1)-X(3)	3.492 (5)	3.487 (5)
X(1)-X(4)	3.482 (5)	3.515 (5)
X(2)-X(3′)	3.516 (5)	3.478 (5)
X(2)-X(4′)	3.507 (5)	3.490 (5)
X(3)-X(4′)	3.493 (5)	3.481 (5)
av X-X	3.497	3.493

Table VIII. Angles (Deg) within the $(Mo_6Cl_7S)Cl_6^{3-}$ Cluster of $(C_5H_5NH)_3[(Mo_6Cl_7S)Cl_6]$

	c sites	b sites
Mo(2)-Mo(1)-Mo(3)	60.03 (4)	59.79 (5)
Mo(2)-Mo(1)-Mo(3′)	60.09 (4)	60.25 (5)
Mo(2′)-Mo(1)-Mo(3)	60.04 (5)	60.24 (5)
Mo(2′)-Mo(1)-Mo(3′)	59.64 (4)	59.97 (5)
Mo(1)-Mo(2)-Mo(3)	59.95 (4)	60.24 (5)
Mo(1)-Mo(2)-Mo(3′)	60.19 (5)	59.86 (4)
Mo(1′)-Mo(2)-Mo(3)	60.08 (4)	60.13 (4)
Mo(1′)-Mo(2)-Mo(3′)	59.61 (4)	60.14 (5)
Mo(1)-Mo(3)-Mo(2)	60.02 (4)	59.98 (5)
Mo(1)-Mo(3)-Mo(2′)	60.35 (4)	59.62 (5)
Mo(1′)-Mo(3)-Mo(2)	60.29 (3)	59.90 (4)
Mo(1′)-Mo(3)-Mo(2′)	59.73 (5)	59.90 (5)
av Mo-Mo-Mo	60.00	60.00
Mo(1)-X(1)-Mo(2)	63.85 (10)	63.30 (9)
Mo(1)-X(1)-Mo(3)	63.88 (10)	63.57 (9)
Mo(2)-X(1)-Mo(3)	63.76 (10)	63.40 (9)
Mo(1)-X(2)-Mo(2)	63.35 (9)	63.42 (9)
Mo(1)-X(2)-Mo(3′)	63.60 (9)	63.50 (9)
Mo(2)-X(2)-Mo(3′)	63.47 (10)	63.68 (9)
Mo(1′)-X(3)-Mo(2)	63.68 (9)	63.66 (9)
Mo(1′)-X(3)-Mo(3)	63.26 (10)	63.89 (10)
Mo(2)-X(3)-Mo(3)	63.29 (8)	63.68 (10)
Mo(1)-X(4)-Mo(2′)	63.63 (9)	63.21 (9)
Mo(1)-X(4)-Mo(3)	63.24 (8)	63.23 (9)
Mo(2′)-X(4)-Mo(3)	63.43 (9)	63.51 (9)
av Mo-X-Mo	63.54	63.50
X(1)-Mo(1)-X(2)	90.3 (1)	90.1 (1)
X(1)-Mo(1)-X(4)	89.9 (1)	90.1 (1)
X(2)-Mo(1)-X(3′)	90.2 (1)	89.8 (1)
X(3′)-Mo(1)-X(4)	89.3 (1)	89.7 (1)
X(1)-Mo(2)-X(2)	89.9 (1)	90.2 (1)
X(1)-Mo(2)-X(3)	90.2 (1)	89.9 (1)
X(2)-Mo(2)-X(4′)	89.9 (1)	89.8 (1)
X(3)-Mo(2)-X(4′)	89.7 (1)	89.9 (1)
X(1)-Mo(3)-X(3)	89.9 (1)	90.1 (1)
X(1)-Mo(3)-X(4)	89.8 (1)	90.3 (1)
X(2′)-Mo(3)-X(3)	90.0 (1)	89.8 (1)
X(2′)-Mo(3)-X(4)	90.0 (1)	89.4 (1)
av X-Mo-X	89.9	89.9
X(1)-Mo(1)-Cl(1)	91.6 (2)	90.0 (1)
X(2)-Mo(1)-Cl(1)	91.7 (1)	91.1 (1)
X(3′)-Mo(1)-Cl(1)	92.9 (1)	94.4 (2)
X(4)-Mo(1)-Cl(1)	92.5 (1)	93.2 (1)
X(1)-Mo(2)-Cl(2)	91.3 (1)	91.2 (1)
X(2)-Mo(2)-Cl(2)	93.1 (1)	91.6 (1)
X(3)-Mo(2)-Cl(2)	90.9 (1)	92.9 (1)
X(4′)-Mo(2)-Cl(2)	93.5 (1)	92.5 (1)
X(1)-Mo(3)-Cl(3)	92.4 (1)	90.7 (1)
X(2′)-Mo(3)-Cl(3)	91.9 (1)	93.6 (1)
X(3)-Mo(3)-Cl(3)	92.3 (1)	92.3 (2)
X(4)-Mo(3)-Cl(3)	91.9 (1)	92.6 (1)
av X-Mo-Cl	92.2	92.2

Table IX. Average Bond Distances (Å) in Selected Mo_6X_8 Cluster Compounds

	Mo-Mo	$Mo-X_b$	ref
$(Mo_6Cl_8)Cl_{4/2}Cl_2$	2.607 (2)	2.471 (2)	8
$Hg[(Mo_6Cl_8)Cl_6]$	2.62 (1)	2.48 (2)	42
$(Mo_6Cl_7Se)Cl_{6/2}$	2.616 (1)	2.495 (1)	43
$(C_5H_5NH)_3[(Mo_6Cl_7S)Cl_6]$	2.606 (2)	2.474 (4)	this work
	2.601 (2)	2.472 (4)	
$(C_5H_5NH)_3[(Mo_6Cl_7S)Cl_6]\cdot 3(C_5H_5NH)Cl$	2.610 (2)	2.475 (5)	this work
Mo_6S_8	2.780	2.439	6
$PbMo_6S_8$	2.705 (3)	2.455 (9)	5

nonhydrogen atoms of the pyridinium cation were indistinguishable, they were labeled R1–R6). Since the sum of the van der Waals radii of nitrogen and chlorine is 3.30–3.45 Å, these contacts may reflect the presence of weak hydrogen bonds.[40] Neither Cl,i nor Cl,is has any other neighbors (excluding pyridinium hydrogens) closer than 3.5 Å. There is no significant contact (<3.5 Å) of the cluster with the pyridinium cations.

---

(40) Pimentel, G. C.; McClellan, A. L. "The Hydrogen Bond", 1st ed.; W. H. Freeman: San Francisco, CA, 1960; Chapter 9.

Table X. Average Mo-L Bond Lengths (Å) and Bond Orders in Selected $(Mo_6X_8)L_6$ Cluster Compounds

compd	L	$Mo-L_t$	$Mo-L_{tt}$[a]	est Mo-L[b]	av bond order[c]
$(C_5H_5NH)_3[(Mo_6Cl_7S)Cl_6]$	Cl	2.454 (4)		2.286	0.52
$(C_5H_5NH)_3[(Mo_6Cl_7S)Cl_6]\cdot 3(C_5H_5NH)Cl$	Cl	2.456 (3)		2.286	0.52
$(Mo_6Cl_8(Cl_2Cl_{4/2}$[8]	Cl	2.379 (1)	2.494 (1)	2.286	0.53
$(Mo_6Br_8)Br_4(H_2O)_2$[9]	Br	2.587 (2)		2.436	0.51
	H_2O	2.191 (18)		1.956	
$Cs_2[(Mo_6Cl_8)Br_6]$[44]	Br	2.59 (1)		2.436	0.55
$(Mo_6Cl_7Se)Cl_{6/2}$[43]	Cl		2.514 (1)	2.286	0.42

[a] L_{tt} = terminal ligand shared with neighboring cluster. [b] Estimated by adding Pauling covalent radius of nonmetal[45] to Pauling metallic radius for molybdenum.[46] [c] Calculated from Pauling's formula: bond order = 10[(est Mo-L) – (Mo-L)]/0.6.

In the structure of $(pyH)_3[(Mo_6Cl_7S)Cl_6]$, the $(Mo_6Cl_7S)Cl_6^{3-}$ clusters again occupy the edge centers and body center of the monoclinic unit cell (b and c sites, $\bar{1}$ site symmetry), and the 12 pyridinium cations occupy general cell positions. The clusters on the b and c sites are crystallographically independent. The arrangement is such that there are no significant interactions between the clusters and the pyridinium cations.

The $(Mo_6Cl_7S)Cl_6^{3-}$ cluster of $(pyH)_3[(Mo_6Cl_7S)Cl_6]\cdot 3pyHCl$ is illustrated in Figure 4. The structure of this cluster is indistinguishable from that of a derivative of $(Mo_6Cl_8)Cl_6^{2-}$ with an octahedron of bonded molybdenum atoms, eight face-bridging ligands, and six terminal chlorides. The labels used in Figure 4 correspond to atom labels used for the interatomic distances and angles of both compounds, listed in Tables VI–VIII.[41]

Inspection of Tables VI and VII reveals that there are small but statistically significant variations among corresponding distances within the three $(Mo_6Cl_7S)Cl_6^{3-}$ clusters. The maximum difference among the Mo–Mo distances is only 0.023 Å. As shown in Table IX, the average Mo–Mo bond lengths for the three $Mo_6Cl_7S^{3+}$ clusters fall in a narrow range and are in good agreement with the values observed for the isoelectronic $Mo_6Cl_8^{4+}$ clusters of Mo_6Cl_{12} and $Hg[(Mo_6Cl_8)Cl_6]$[42] and the isoelectronic $Mo_6Cl_7Se^{3+}$ cluster of $Mo_6Cl_{10}Se$.[43]

The average $Mo–X_b$ bond lengths of the three $Mo_6Cl_7S^{3+}$ clusters are from 2.472 to 2.475 Å, in excellent agreement with the $Mo–Cl_b$ bond lengths of the isoelectronic $Mo_6Cl_8^{4+}$ cluster compounds.

So that the bridging sulfide could be distinguished from the bridging chlorides, the $Mo–X_b$ bond lengths of the independent bridging ligands were carefully compared. Pinpointing the sulfide is problematic for two reasons. It may be disordered over all the bridging ligand sites, as has been observed with selenide in the $Mo_6Cl_7Se^{3+}$ cluster of $(Mo_6Cl_7Se)Cl_3$.[43] Second, sulfide and chloride are nearly equivalent X-ray scatterers. However, if sulfide is ordered, or only partially disordered, the $Mo–X_b$ bond distances should serve to distinguish it from chloride since the $Mo–S_b$ bond in the Chevrel phases is 0.02–0.04 Å shorter than the $Mo–Cl_b$ bond of α-molybdenum(II) chloride.[6,8]

The two crystallographically independent bridging ligands of $(pyH)_3[(Mo_6Cl_7S)Cl_6]\cdot 3pyHCl$ have equivalent $Mo–X_b$ bond lengths, so the sulfide's location cannot be discerned in this compound.

In $(pyH)_3[(Mo_6Cl_7S)Cl_6]$, the Mo–X bonds of the X3b and X1c bridging ligands are the three shortest bonds in the b and c clusters, respectively. The average $Mo–X_b$ bond lengths of these two ligands are significantly shorter than the average bond lengths of the remaining bridging ligands. Thus, sulfide is disordered over only two of the eight bridging ligand sites in each cluster of $(pyH)_3[(Mo_6Cl_7S)Cl_6]$. This conclusion is supported by the observation that the Mo–Mo distances of the octahedral faces capped by X3b and X1c are the shortest Mo–Mo distances in both clusters, viz. Mo(1)–Mo(2), Mo(1)–Mo(3), and Mo(2)–Mo(3).

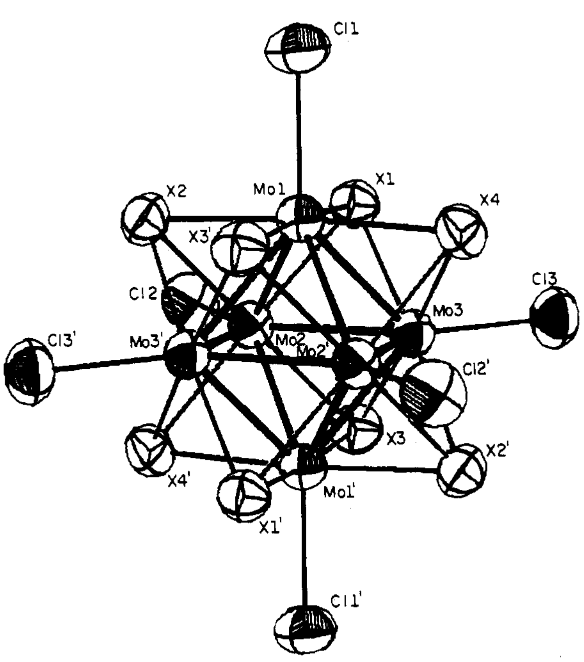

Figure 4. Labeled perspective view of the 50% probability thermal ellipsoids of the $(Mo_6Cl_7S)Cl_6^{3-}$ cluster as it occurs in both $(pyH)_3[(Mo_6Cl_7S)Cl_6]$ and $(pyH)_3[(Mo_6Cl_7S)Cl_6]\cdot 3pyHCl$.

The $Mo–Cl_t$ bond lengths of the three $(Mo_6Cl_7S)Cl_6^{3-}$ clusters are equivalent and as shown in Table X seem anomalously long when compared to the $Mo–Cl_t$ bonds of Mo_6Cl_{12}. Interestingly, the $Mo–Cl_t$ bond length of $(Mo_6Cl_7S)Cl_6^{3-}$ is nearly equal to the weighted average of the two $Mo–Cl_t$ and the four $Mo–Cl_{tt}$ bond lengths of Mo_6Cl_{12}. Furthermore, Table X indicates that the apparent bond order[45] of the $Mo–Cl_t$ bond of $(Mo_6Cl_7S)Cl_6^{3-}$ is commensurate with the average $Mo–L_t$ bond orders of other $(Mo_6X_8)L_6$ clusters. Thus, the apparent strength of the bonding interaction between the molybdenum atoms and the terminal ligands is a constant for all these $(Mo_6X_8)L_6$ clusters. Considered in this light, the $Mo–Cl_t$ bond length of the $(Mo_6Cl_7S)Cl_6^{3-}$ cluster is reasonable.

Conclusion

The discrete chloride sulfide cluster $Mo_6Cl_7S^{3+}$ has been prepared by substitution of sulfide into $Mo_6Cl_8^{4+}$. Members

---

(41) Busing, W. R.; Martin, K. O.; Levy, H. A. "ORFFE, A Fortran Crystallographic Function and Error Program", US AEC Report ORNL-TM-306; Oak Ridge National Laboratory: Oak Ridge, TN, 1964.

(42) Von Schnering, H. G. *Z. Anorg. Allg. Chem.* **1971**, *385*, 75.

(43) Perrin, C.; Sergent, M.; Le Traon, F.; Le Troon, A. *J. Solid State Chem.* **1978**, *25*, 197.

(44) Healy, P. C.; Kepert, D. L.; Taylor, D.; White, A. H. *J. Chem. Soc., Dalton Trans.* **1973**, 646.

(45) Pauling, L. "The Nature of the Chemical Bond", 3rd ed.; Cornell University Press; Ithaca, NY, 1960; p 224.

(46) Reference 45, p 256.

of the $Mo_6Cl_{8-n}S_n$ series with high-sulfide contents can be similarly prepared, providing incentive for work currently under way aimed at synthesizing discrete Mo_6S_8 cluster derivatives.

The substitution of a single chloride by sulfide dramatically alters the electronic structure of the Mo_6X_8 cluster. One indicator of the change in electronic structure is the change in color going from $Mo_6Cl_8^{4+}$ (yellow) to $Mo_6Cl_7S^{3+}$ (red). Another indicator is the decreased difference between the XPS binding energies of the bridging and terminal chlorides in $Mo_6Cl_7S^{3+}$ (1.8 eV) in comparison to $Mo_6Cl_8^{4+}$ (2.2 eV).

In contrast to the differences evident in the electronic structure, the Mo-Mo and Mo-Cl bond distances in $Mo_6Cl_7S^{3+}$ are nearly identical with those of $Mo_6Cl_8^{4+}$. However, subtle differences in bond lengths in the structure of $(pyH)_3[(Mo_6Cl_7S)Cl_6]$ permit the crystallographic sites occupied by the bridging sulfide to be located.

Acknowledgment. We thank the National Science Foundation for a grant to the Department of Chemistry for the purchase of the photoelectron spectrometer used in this research.

Registry No. $(pyH)_3[(Mo_6Cl_7S)Cl_6]$, 75085-32-4; $(pyH)_3[(Mo_6Cl_7S)Cl_6]\cdot 3pyHCl$, 75069-92-0; Mo_6Cl_{12}, 11062-51-4; $[(n\text{-}C_4H_9)_4N]_2[(Mo_6Cl_8)Cl_6]$, 12367-12-3; $(pyH)_2[(Mo_6Cl_8)Cl_6]$, 80754-08-1.

Supplementary Material Available: Listings of structure factor amplitudes, anisotropic temperature factors, and C-C or C-N bond distances (26 pages). Ordering information is given on any current masthead page.

Contribution from the Institut für Physikalische und Theoretische Chemie der Universität Tübingen, 7400 Tübingen, West Germany, and the Anorganisch-Chemisches Institut der Universität Göttingen, 3400 Göttingen, West Germany

Gas-Phase Molecular Structure of Sulfur Tetrafluoride Methylimide, $CH_3N{=}SF_4$. An NMR, Electron Diffraction, Microwave, and ab Initio Study

HORST GÜNTHER, HEINZ OBERHAMMER,* RÜDIGER MEWS, and INGO STAHL

Received July 14, 1981

The molecular structure of $CH_3N{=}SF_4$ in the gas phase has been determined by joint analysis of electron diffraction and microwave spectroscopy data. A strongly distorted trigonal-bipyramidal structure with the double bond in equatorial position and the methyl group pointing in axial direction has been obtained, confirming the interpretation of the NMR spectra. Geometric parameters are compared to the ab initio results for $HN{=}SF_4$, and the bond angles around the sulfur atom are correlated with the electronic structure of the S=N π bond. The temperature dependence of the NMR spectra is discussed.

Introduction

Molecular structures and bonding properties of pentacoordinate sulfur(VI) compounds are particularly interesting. For a long time $O{=}SF_4$[2] was the only known member in this class of molecules. Only recently the "isoelectronic" sulfur tetrafluoride imides $RN{=}SF_4$[3-6] and methylene sulfur tetrafluoride $CH_2{=}SF_4$[7] were synthesized. Whereas $O{=}SF_4$[8] and $CH_2{=}SF_4$[9,10] have been studied in greater detail, only little is known about the various sulfur tetrafluoride imides.[11] In this study we report the NMR spectra and gas-phase structure investigation for $CH_3N{=}SF_4$. For this molecule only the combination of electron diffraction data and rotational constants allows a reliable structure determination without constraints for the bond distances. A structure determination from electron diffraction data alone would require serious geometric constraints due to the high correlations between various bond distances.

Experimental Section

CH_3NSF_4 was prepared according to the literature method.[5] It was separated from impurities (CH_3F, NSF_3) by fractional condensation (-120, -196 °C) under vacuum. The pure compound (checked by IR and NMR spectroscopy) remained in the -120 °C trap. The compound is very sensitive to moisture; it readily hydrolyses to give CH_3NSOF_2 and CH_3NHSF_5. NMR spectra were recorded with a Bruker E 60, ^{19}F NMR spectra with a Bruker WH 360 FT (at the University of Bremen), and ^1H spectra also with a Varian XL 200 (at the Institute for Organic Chemistry, University of Göttingen).

Table I. Details of Electron Diffraction Experiment

camera dist, cm	50	25
nozzle diameter, mm	0.2	0.2
sample temp, °C	-40	-42
nozzle temp, °C	10	10
camera pressure, torr	2×10^{-5}	10^{-5}
exposure time, s	8-25	25-60
electron wavelength, Å	0.048 87 (1)	0.048 85 (1)
s range, Å^{-1} [a]	1.6-17	10-35

[a] $s = (4\pi/\lambda) \sin (\theta/2)$. λ = electron wavelength; θ = scattering angle.

Table II. Rotational Constants (GHz) for $CH_3N{=}SF_4$

	A	*B*	*C*
B^i_0	3.34307 (3)	2.14935 (1)	1.87452 (1)
B^i_z	3.34126 (28)	2.14865 (11)	1.87380 (11)
B^i_z(calcd)	3.34144	2.14871	1.87384

The electron diffraction intensities were recorded with a Balzers diffractograph KD-G2[12] at two camera distances, 50 and 25 cm. Details of the experiment are listed in Table I. (Throughout this paper 1 Å = 100 pm, 1 torr = 101.325/760 kPa, and 1 cal = 4.184 J.) The electron wavelength was determined by ZnO powder dif-

---

* To whom correspondence should be addressed at the Institut für Physikalische und Theoretische Chemie der Universität Tübingen.

(1) Preliminary geometric parameters, based on electron diffraction data only, have been cited by O. Glemser and R. Mews, *Angew. Chem.*, **92**, 904 (1980); *Angew. Chem., Int. Ed. Engl.*, **19**, 883 (1980).

(2) O. Ruff and H. Jones, *Naturforsch. Med. Deutschland 1939-44*, **23**, 182; H. Jones, *Z. Anorg. Allg. Chem.*, **265**, 273 (1951).

(3) C. W. Tullock, D. D. Coffman, and E. L. Muetterties, *J. Am. Chem. Soc.*, **86**, 357 (1964).

(4) (a) I. Stahl, R. Mews, and O. Glemser, *J. Fluorine Chem.*, **7**, 55 (1976); (b) *Angew. Chem.*, **92**, 393 (1980); *Angew Chem., Int. Ed. Engl.*, **19**, 408 (1980).

(5) R. Mews, *Angew. Chem.*, **90**, 561 (1978); *Angew. Chem., Int. Ed. Engl.*, **17**, 530 (1978).

(6) D. D. Des Marteau and K. Seppelt, *Angew. Chem.*, **92**, 659 (1980); *Angew. Chem., Int. Ed. Engl.*, **19**, 643 (1980).

(7) G. Kleemann and K. Seppelt, *Angew. Chem.*, **90**, 547 (1978); *Angew. Chem., Int. Ed. Engl.*, **17**, 516 (1978).

0020-1669/82/1321-1872$01.25/0